Text S1

1. MATERIALS AND METHODS

1.1. Radiative transfer modeling

In a backward Monte Carlo (BMC) simulation, rays are emitted from the detector and traced to the source. The emitted rays are given an angular distribution specific to the type of detector. For example, a planar irradiance sensor, simulating a plating coral, has a cosine response to incoming radiance. Therefore, to simulate a cosine detector, the rays are emitted from the detector in an angular pattern derived from the cosine response of the detector and each ray emitted is given an initial weight of one. An emitted ray is then traced using the same techniques as in the forward Monte Carlo simulation. However, it is much more likely that an emitted ray will find its way from a small detector to the sky than from the sky to a small detector at a particular location. The principle of electromagnetic reciprocity guarantees that if a ray from the detector reaches the sky traveling in a particular direction, then a ray leaving the sky in the opposite direction would retrace the ray path back to the detector. If a ray reaches the sky, it is given the final weight of the sky radiance in that direction. The accumulated weights of the rays leaving the detector (coral) and reaching the sky then give the fraction of sky radiance in each direction that would reach the coral. BMC simulation is numerically most efficient for an extended source (i.e., the sky in this case) and a localized detector (a detector of a particular coral morphology, substrate angle and depth on the reef).

The reef topography in Fig. 1a of the main text consists of the typical coral reef profile with a horizontal reef top, reef slope, and a vertical reef wall, while Fig. 1b of the main text shows the same reef but with a continuation of the sloping reef into the lower mesophotic depths. The reef is infinite in extent in the ± ŷ directions, and the top and wall are half planes. The depths and horizontal locations of the top-slope and slope-wall boundaries are inputs to the Monte Carlo code. If the top-slope boundary is placed to the right of the slope-wall boundary, an overhanging area can be simulated. The sun can be placed at any polar, azimuthal angles (2_{sun}, N_{sun}), so that the reef wall can be either in direct sunlight or in its own shadow. The detector with its unique morphology can be placed at any location on the surface of the reef or in the water column. We present results for four detector geometries, which can be on the reef top, slope, or wall. PAR_{hs} denotes PAR as measured by a hemispherical detector (mounding coral), PAR_{cos} denotes PAR as measured by a plane irradiance (cosine-response) detector (plating coral), and PAR_{br} denotes PAR averaged over the surface area of a branching coral. In each case, the detector is placed on the reef surface and is oriented facing outward from reef surface. In addition, we present results for PAR as computed by scalar irradiance detector placed just in front of the coral surface; this is denoted by PAR_o. Note that $PAR_o > PAR_{hs}$ because PAR_{hs} sees only one-half of the sphere of all directions. $PAR_{hs} > PAR_{cos}$ because of the cosine weighing of a plane irradiance detector. PAR_{br} is less than the other measures of PAR because the same incident energy is spread out over a larger detector area, namely the surface area of the branching coral.

Ambient E_d in air just above the sea surface, was modelled as in HydroLight (https://www.numopt.com/hydrolight.html), which uses the RADTRAN sky irradiance model

(Gregg & Carder 1990) combined with a normalized sky irradiance model (Harrison & Coombes 1988) to generate a sky irradiance distribution that reproduces the RADTRAN E_d. The RADTRAN inputs used a year-day of 183, marine aerosol from the US Navy aerosol model which results in an aerosol optical thickness of 0.261 at 550 nm for a clear sky, a wind speed of 5 m s^{-1}, sea level pressure of 29.9 in Hg, relative humidity of 80%, precipitable water of 2.5 cm, visibility of 15 km, and total ozone of 300 Dobson units. The IOP inputs into the BMC code are the wavelength-dependent total (water plus other constituents) absorption, scattering, and backscattering spectra, including wavelength specific representation for each reef location (i.e., reef top, reef slope and vertical reef wall). These IOPs were the averages of measurements for the back reef, fringing reef and fore reef locations described in Russell et al. (2019). The Russell et al. (2019) measurements were obtained from coral reefs in Hawaii, Australia, Guam and Palau using as part of a validation program for airborne satellite imagery from back, fringing, fore and patch reefs using an optical instrument package consisting of a calibrated ac-s spectrophotometer, a VSF-3 scattering meter, a DH4 data logger and a SeaBird SBE37 CTD. Water samples were collected during casts using a SeaBird SBE16 pump for the ac-s measurements. The spectral absorption and scattering measurements revealed that the IOPs on nearshore coral reefs are significantly influenced by elevated concentrations of colored dissolved organic matter (CDOM) and mineral particles, compared to open-ocean waters, where the absorption and scattering properties are determined primarily by phytoplankton (e.g., Boss & Zaneveld 2003). Thus, the use of open-ocean bio-optical models or measurements is highly likely to be inappropriate for modeling in-water optics over, or close to, coral reef habitats. The Russell et al. (2019) data are at 1 nm resolution but were subsampled to 10 nm resolution to match the BMC code that was run from 400 to 700 nm at 10 nm resolution to compute the spectral irradiance for the different sensor types. The spectral irradiances (in energy units of W m^{-2} nm^{-1}) were then converted to PAR (quantum units of µmol quanta m^{-2} s^{-1}).

The ratio of backscattering to total scattering was used to determine a wavelength-dependent Fourier-Forand phase function, as it is done in HydroLight. The water was assumed to be homogeneous, so that the water IOPs do not vary with depth or horizontal location. The wind speed of 5 m s^{-1} was used to determine the random slopes of sea-surface wave facets using the Cox & Munk (1954) wave slope-wind speed equations. The reef top, slope, and wall were assumed to be Lambertian reflectors, so that only the spectral irradiance reflectance of the reef surfaces need be specified. Those values come from averages of direct measurements (e.g., Lesser & Mobley 2007).

1.2. Generating radiance distributions for branching sensor calculations (PAR_{br})

In order calculate the branching sensor response, a full directional radiance distribution is required, The BMC model provided planar and scalar irradiances for each modelled scenario, these were used to construct ‘plausible’ full radiance distributions using modified infinite depth ’open water’ radiance distributions from HydroLight. The directional radiance distributions were tabulated according to the same spherical quad-structure as HydroLight, in 30 10 nm wide bands from 400-700 nm.

The design rationale was that at some distance from the reef slope or wall, the plane-parallel HydroLight radiance distribution would be accurate. Moving closer the reef, the 'open water' radiance distribution would be modified by the influence of the reef, and this can be approximated by two simple mechanisms: 1) the overall radiances would be reduced by a scaling factor applied uniformly over all wavelengths and directions, 2) there would be 'wall factor' that meant the change in radiance would be at a minimum for directions looking perpendicular to the reef surface (i.e. looking maximally 'far away' from the reef surface), but looking increasingly toward the direction tangential to the surface the influence of the wall on the light field would increase. It was assumed that this wall effect would be a function of the cosine of the angle to the perpendicular to the reef surface and also act to increase or decrease the radiance uniformly for all wavelengths. Finally, the radiance for all view directions onto the reef surface is defined by the assumption the surface is Lambertian and has the spectral reflectance as used in the Monte Carlo model. This radiance is therefore set by the planar irradiance onto the surface as known from the Monte Carlo modelling. The spectral radiance $L(i,\lambda)$ is defined in 434 'quads', with i = 1,2...434 (which are in the same arrangement used in HydroLight, except here we refer to them by a single index), and is:

$$L(i,\lambda) = \begin{cases} L_{\mathrm{WALL}}(i,\lambda) & \text{if } \boldsymbol{v}(i)\cdot\boldsymbol{n} \geq 0 \\ L_{\mathrm{H}}(i,\lambda)[s + w(1 - |\boldsymbol{v}(i)\cdot\boldsymbol{n}|)] & \text{if } \boldsymbol{v}(i)\cdot\boldsymbol{n} < 0 \end{cases} \quad (1)$$

where **n** is the unit length normal vector perpendicular to the reef surface (pointing off it) and **v**(i) is a unit length vector in the direction of light propagation represented by the centre of quad i.

$L_{\mathrm{WALL}}(i,\lambda)$ is the radiance leaving the wall surface, given by,

$$L_{\mathrm{WALL}}(i,\lambda) = E_{\mathrm{p}}(\lambda) \times R(\lambda)/\pi \quad (2)$$

Here $R(\lambda)$ is the diffuse reflectance of the surface and $E_{\mathrm{p}}(\lambda)$ is the spectral planar irradiance incident on the surface. The latter can be calculated after the opposite hemisphere of $L(i,\lambda)$ is defined, so in practice Eq. 1 is first evaluated for indices where **v**(i) • **n** < 0.

$L_{\mathrm{H}}(i,\lambda)$ is the radiance calculated by HydroLight for the corresponding depth IOPs and solar position. The two values s and w must be deduced for every location and solar position in order to produce a distribution $L(i,\lambda)$ that gives the same PAR hemispherical scalar irradiance ($\mathrm{PAR_{hs}}$) and PAR planar irradiance ($\mathrm{PAR_{cos}}$) as derived from the Monte Carlo model. Fortunately, since s and w act in a spectrally uniform way, they can be calculated directly from PAR irradiances, plus a kind of pseudo-irradiance parameter denoted Ex below, which is like planar irradiance but calculated with a cosine-squared factor rather than a cosine factor. The expressions are,

$$w = \frac{E_{\mathrm{o}}^{\mathrm{H}} E_{\mathrm{p}}^{\mathrm{MC}} - E_{\mathrm{p}}^{\mathrm{H}} E_{\mathrm{o}}^{\mathrm{MC}}}{E_{\mathrm{p}}^{\mathrm{H}} E_{\mathrm{p}}^{\mathrm{H}} - E_{\mathrm{o}}^{\mathrm{H}} E_{\mathrm{x}}^{\mathrm{H}}} \quad (3)$$

$$s = \frac{E_{\mathrm{o}}^{\mathrm{MC}} - w(E_{\mathrm{o}}^{\mathrm{H}} - E_{\mathrm{p}}^{\mathrm{H}})}{E_{\mathrm{o}}^{\mathrm{H}}} \quad (4)$$

Note that the symbol E is used, and each term is spectrally integrated PAR in μmol quanta m^{-2} s^{-1}.

The input quantities are,

$E_{\mathrm{p}}^{\mathrm{MC}}$ The planar PAR irradiance onto the reef surface from the Monte Carlo model (PAR_{cos}).

$E_{\mathrm{o}}^{\mathrm{MC}}$ The hemispherical scalar PAR irradiance onto reef reef surface from the Monte Carlo model (PAR_{hs}).

$E_{\mathrm{p}}^{\mathrm{H}}$ The planar PAR irradiance in a direction corresponding to incidence on the reef surface in the open water HydroLight radiance distribution.

$E_{\mathrm{o}}^{\mathrm{H}}$ The hemispherical scalar PAR irradiance in a direction corresponding to incidence on the reef surface in the open water HydroLight radiance distribution.

and,

$$E_x^{\mathrm{H}} = \mathrm{PAR}\left[\sum_{i}^{\boldsymbol{v}(i)\cdot\boldsymbol{n}<0} L_{\mathrm{H}}(i,\lambda)\Omega(i)(\boldsymbol{v}(i)\cdot\boldsymbol{n})^2\right] \quad (5)$$

where PAR[ ] indicates the function to convert the 30 band spectral value into a PAR value of μmol quanta m^{-2} s^{-1}.

With *s* and *w* thus defined the resulting radiance distribution $L(i,\lambda)$ given by Eq. 1 matches both the required planar PAR irradiance and scalar PAR irradiance onto the reef surface, and also has the correct radiance exitant from the reef surface, assuming the surface is Lambertian. In all other other respects, the radiance distribution is very similar to the 'open water' HydroLight solution, as the examples below show.

1.3. Examples of radiance distributions as polar plots

The following polar plots show some examples of the generated radiance distributions and the plane-parallel 'open water' HydroLight distributions they are generated from. Plots are in the x-z plane, i.e. the plane perpendicular to the reef surface, with upward in the plot being the directly upward (z-) direction. Plots are logarithmic in the radial axis.

Shallow locations (10 m and 12 m)

(a) Sun at 30°, location on reef flat at 10 m depth	**(b) Sun at 80° behind slope, location at 12 m depth**
L(550 nm), θ = 30°, φ = 0°, 10 m, back reef IOPs	L(550 nm), θ = 80°, φ = 180°, 12 m, fringe IOPs
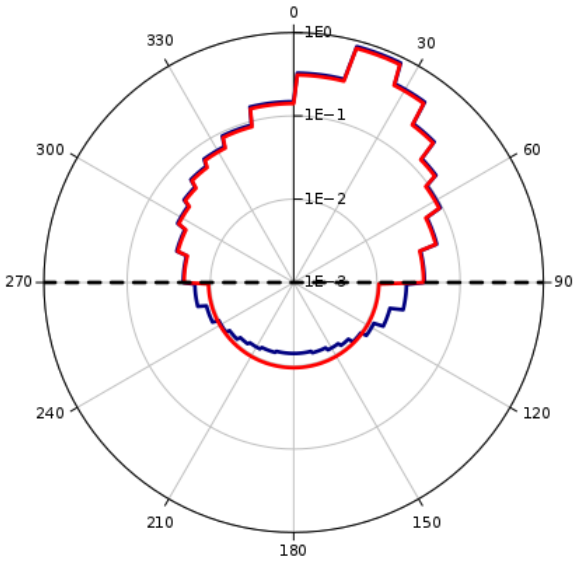	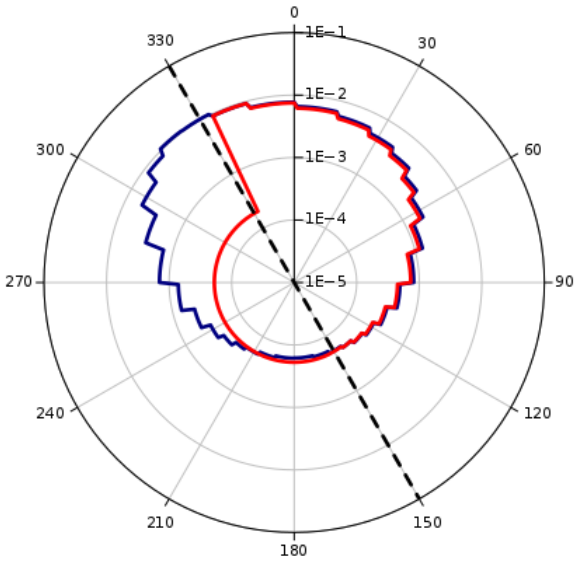

HydroLight 'open water' radiance at 550 nm, $L_H(550)$
modelled radiance distribution at reef surface from Eq. 1, L(550)
reef surface

(a) On the reef flat a HydroLight radiance distribution with finite depth could be directly used, but instead, for comparison, the scheme based on *s* and *w* has been used. Note the light is dominated by the downward solar irradiance. The influence of the surface underneath is negligible and the downwelling part of the radiance distribution is almost the same for the infinitely deep water at the same location.

(b) At 12 m depth with sun at 50° behind the slope the direct illumination direction is shadowed by the slope. However, a large part of the light distribution is already scattered into general downwelling directions and the incident irradiance is matched by the plane-parallel solution in the corresponding hemisphere with minimal modification.

Slope locations at 30 m

(c) Sun at 30° in front of slope, location 30 m depth	**(d) Sun at 50° behind slope, location 30 m depth**
L(550 nm), θ = 30°, φ = 0°, 30 m, fringe IOPs	L(550 nm), θ = 50°, φ = 180°, 30 m, fringe IOPs
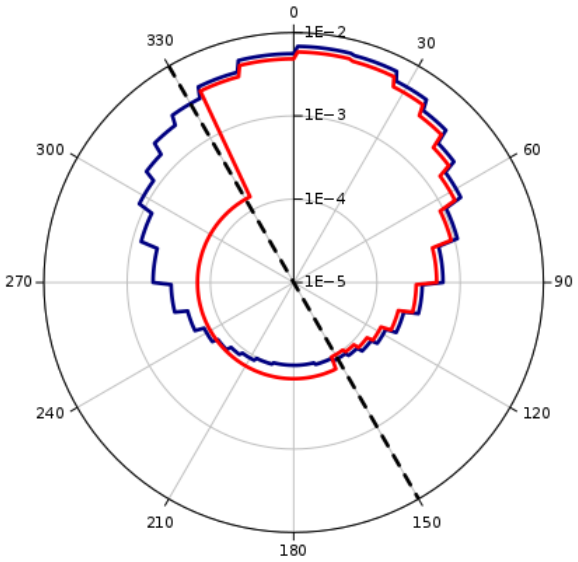	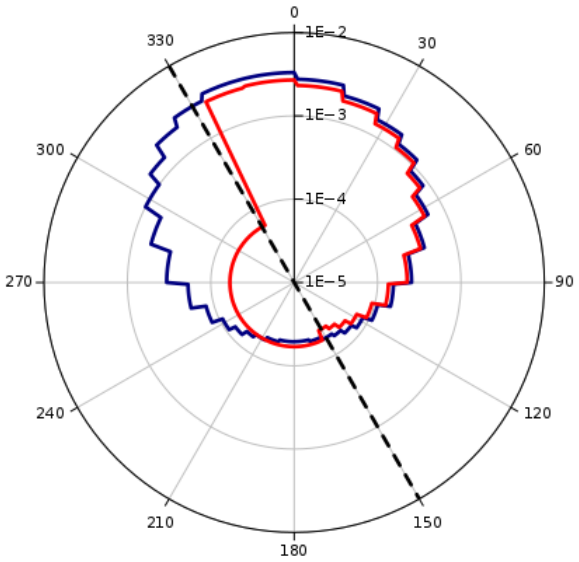

Wall locations at 65 m

(e) Sun at 30° in front of the wall, 65 m depth	**(f) Sun at 50° behind the wall, 65 m depth**
L(550 nm), θ = 30°, φ = 0°, 65 m, fore reef IOPs	L(550 nm), θ = 50°, φ = 180°, 65 m, fore reef IOPs
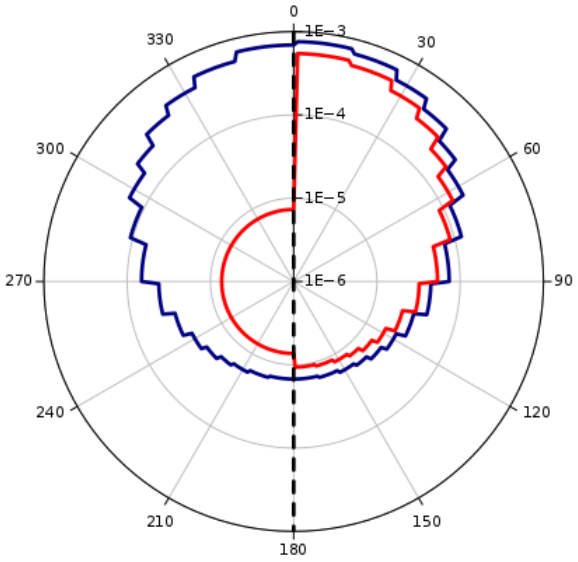	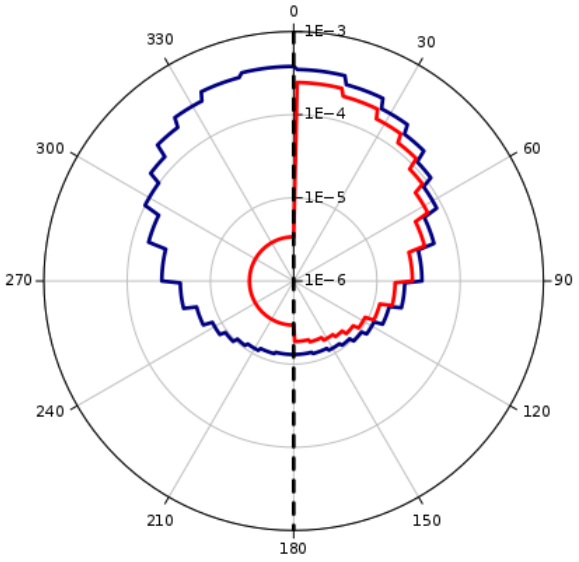

Figure S1. Water-column inherent optical properties (IOPs) and coral reflectance used in the Monte Carlo simulations. Panels (a-c) show the total (including water) absorption (a) and scattering (b) coefficients and backscatter fractions (c) as measured by Russell et al. (2019) for the fore, fringing, and back reef habitats. Panel (d) shows the coral irradiance reflectance. All curves are averages of multiple measurements at different locations from Russell et al. (2019).

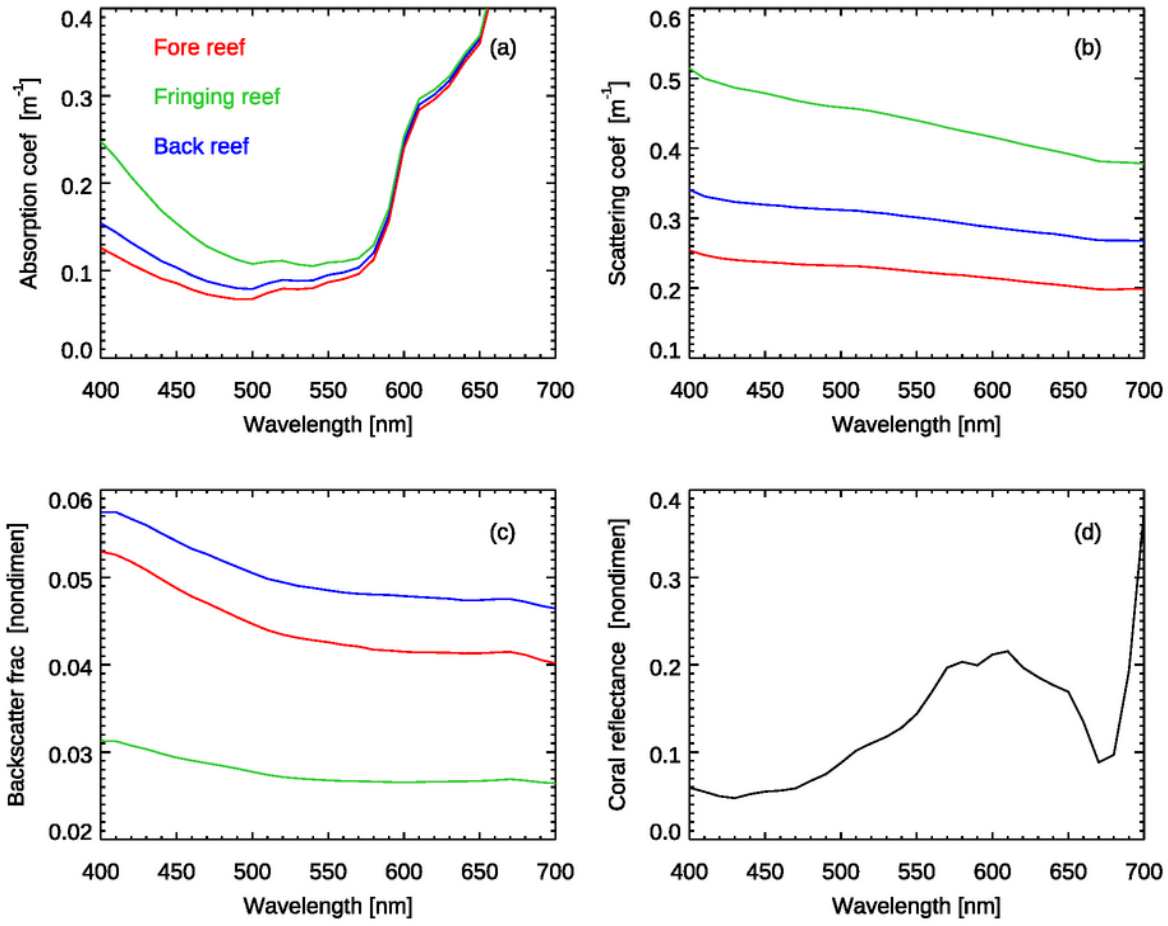

Figure S2. Virtual sensor simulating a branching morphology. The branching shape when illuminated by a radiance distribution at 10 m on the reef flat, with the sun at zenith position such that self-shading within the structure can be seen.

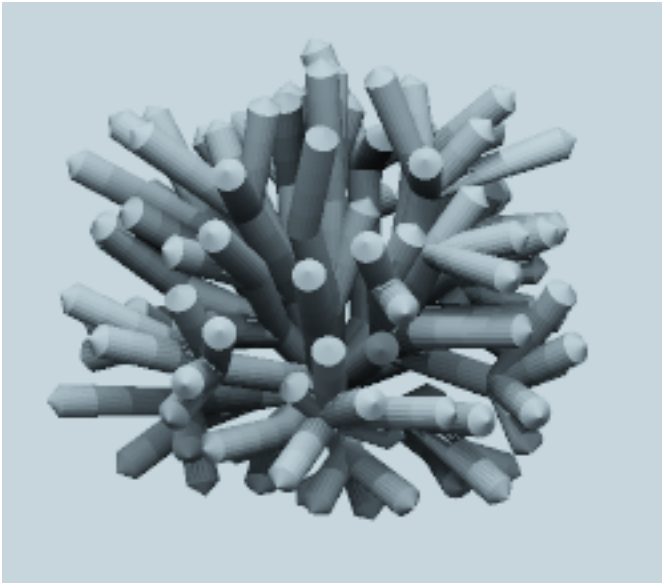

LITERATURE CITED

Boss E, Zaneveld JRV (2003) The effect of bottom substrate on inherent optical properties: evidence of biogeochemical processes. Limnol Oceanogr 48: 346-354 https://doi.org/10.4319/lo.2003.48.1_part_2.0346

Cox C, Munk W (1954) Statistics of the sea surface derived from sun glitter. J Mar Res 13: 198-227

Gregg WW, Carder KL (1990) A simple spectral solar irradiance model for cloudless maritime atmospheres. Limnol Oceanogr 35: 1657-1675 https://doi.org/10.4319/lo.1990.35.8.1657

Harrison AW, Coombes CA (1988) Comparison of model and indirectly measured diffuse sky irradiances of tilted surfaces. Atmosphere-Ocean 26: 193-202 https://doi.org/10.1080/07055900.1988.9649299

Lesser MP, Mobley CD (2007) Bathymetry, water optical properties, and benthic classification of coral reefs using hyperspectral remote sensing imagery. Coral Reefs 26: 810-829 https://doi.org/10.1007/s00338-007-0271-5

Russell BJ, Dierssen HM, Hochberg EJ (2019) Water column optical properties of Pacific coral reefs across geomorphic zones and in comparison to offshore waters. Rem Sens 11: 1757 https://doi.org/10.3390/rs11151757